

Brief Report

# Molecular Dynamics Investigation of the Gasification and Hydrogen Production Mechanism of Phenol in Supercritical Water

Zhigang Liu <sup>1,2</sup>, Liang Wu <sup>1</sup>, Yue Qiu <sup>1</sup>, Fan Liu <sup>1</sup>, Lei Yi <sup>1,\*</sup> and Bin Chen <sup>1,2</sup>

<sup>1</sup> International Institute for Innovation, Jiangxi University of Science and Technology, Ganzhou 341000, China

<sup>2</sup> State Key Laboratory of Multiphase Flow in Power Engineering (SKLMF), Xi'an Jiaotong University, Xi'an 710049, China

\* Correspondence: l-yi@jxust.edu.cn

**Abstract:** Supercritical water gasification is an efficient and clean method for converting biomass into hydrogen-rich gas. Phenol plays a crucial role as an intermediate product in biomass supercritical water gasification, and studying its reaction pathway in supercritical water is essential for understanding the chemical reaction mechanism and optimizing biomass energy conversion processes. In this paper, we investigated the conversion mechanism of phenol gasification and hydrogen production in supercritical water using a combined approach of reactive force field (ReaxFF) and density functional theory (DFT). We determined the decomposition pathways and product distribution of phenol in supercritical water. The calculation results demonstrate that in the supercritical water system, the efficiency of phenol conversion for hydrogen production is approximately 27 times higher than that of hydrogen production through gasification in the pyrolysis state. Moreover, both the carbon conversion rate and hydrogenation rate in the supercritical water system are significantly higher compared to those in the pyrolysis system. Furthermore, we found that the energy in the supercritical system is approximately half that of the pyrolysis system, favoring the ring-opening reactions of phenol and promoting hydrogen production. In contrast, the pyrolysis system produces a greater quantity of aromatic compounds, leading to tar formation and having significant implications for both the reaction process and reactor design. Additionally, we conducted comparative experiments between the supercritical water gasification process and the pyrolysis process to explore the advantages of supercritical water gasification.

**Keywords:** phenol; supercritical water; molecular dynamics; gasification; pyrolysis



check for updates

**Citation:** Liu, Z.; Wu, L.; Qiu, Y.; Liu, F.; Yi, L.; Chen, B. Molecular Dynamics Investigation of the Gasification and Hydrogen Production Mechanism of Phenol in Supercritical Water. *Sustainability* **2023**, *15*, 12880. <https://doi.org/10.3390/su151712880>

Academic Editor: Domenico Licursi

Received: 4 July 2023

Revised: 20 August 2023

Accepted: 24 August 2023

Published: 25 August 2023



**Copyright:** © 2023 by the authors. Licensee MDPI, Basel, Switzerland. This article is an open access article distributed under the terms and conditions of the Creative Commons Attribution (CC BY) license (<https://creativecommons.org/licenses/by/4.0/>).

## 1. Introduction

Climate change is one of the most pressing challenges facing humanity [1]. Since the Industrial Revolution, human activities, such as the combustion of fossil fuels and industrial processes, have emitted significant amounts of carbon dioxide into the atmosphere, thereby becoming the primary cause of climate change. Energy transition is an inevitable aspect of the ongoing advancement of human civilization, and it is imperative for the world to transition towards sustainable energy systems [2]. Consequently, scientists have been actively seeking renewable and sustainable energy sources as gradual replacements for fossil fuels.

Biomass has been recognized as a potential energy source for half of the world's population. Compared to fossil fuels, biomass offers advantages such as renewability, environmental friendliness, and sustainability [3]. Therefore, in the context of the ongoing energy transition, biomass has garnered considerable attention as an alternative energy source. The current primary utilization of biomass as fuel is still direct combustion. Utilizing renewable biomass as a fuel offers advantages in terms of sustainability and long-term supply compared to finite fossil fuels. This helps reduce reliance on fossil fuels and mitigate

energy supply instability. However, the direct combustion of biomass generates aerosols, such as particulate matter, and gas emissions, including nitrogen oxides and sulfur dioxide. These emissions have potential negative impacts on air quality and the environment [4], particularly in the absence of proper emission control measures. However, the application of supercritical water gasification technology avoids the aforementioned issues.

The critical temperature of water,  $T = 374\text{ }^{\circ}\text{C}$ , and critical pressure,  $P = 22.1\text{ MPa}$ , mark the boundary at which water undergoes a phase transition into a state known as supercritical water [5]. Supercritical water gasification technology is a high-temperature, high-pressure chemical reaction process that utilizes supercritical water to convert organic substances into gases. By employing supercritical water gasification technology, biomass gasification can be converted into hydrogen-rich gas. Hydrogen gas, as an ideal fuel, offers a promising solution to address the energy crisis. Moreover, the combustion of hydrogen does not produce any polluting gases. However, during the process of biomass supercritical water gasification, complete direct conversion to hydrogen does not occur. Instead, numerous intermediate products are generated, which can have an impact on the overall efficiency of hydrogen production. Research has indicated that phenol is recognized as a significant intermediate product in biomass supercritical water gasification. Specifically, biomass undergoes a series of chemical reactions in supercritical water, including deoxygenation, dehydration, decarboxylation, and deamination, resulting in the formation of numerous intermediate products [6]. Among these, phenol can be generated through catalytic cracking, gasification, and hydrolysis reactions of aromatic compounds present in biomass, such as lignin and cellulose, under high-temperature and -pressure conditions. Additionally, phenol can further undergo transformations into other compounds, including phenols, alcohols, and ketones, ultimately giving rise to gaseous products such as hydrogen and liquid products such as phenol derivatives and phenolic resins [7]. Biomass gasification has been identified as a potential method for hydrogen production. Therefore, investigating the reaction mechanism of phenol gasification in supercritical water for hydrogen production plays a pivotal role in biomass energy conversion processes.

The production of hydrogen from phenol has attracted widespread attention among researchers. Walid Nabgan et al. [8] conducted a kinetic study on phenol steam reforming over a Ni-Co/ZrO<sub>2</sub> catalyst, utilizing a reaction rate model developed based on Langmuir-Hinshelwood and Eley-Rideal mechanisms to model the chemical reaction. The results revealed that the surface reaction was the rate-limiting step for phenol steam reforming using the Ni-Co/ZrO<sub>2</sub> catalyst. Amir Mosayebi et al. [9] investigated the kinetics and conducted experimental research on hydrogen production from phenol steam reforming using a Ni-Rh/MgO catalyst. The results indicated that higher temperatures on the catalyst surface favored the catalytic performance of phenol conversion, as well as the production of H<sub>2</sub> and carbon monoxide. These research findings provide valuable insights into the pyrolysis and gasification processes of phenol. However, the current gasification methods encounter certain challenges. For instance, they involve significant energy consumption during the gasification process, require pre-treatment of the feedstock prior to the reaction, and result in the generation of substantial by-products, leading to difficulties in product separation. Nevertheless, Zhang et al. [10] employed ReaxFF-MD to convert abundant phenolic compounds present in the thermochemical conversion wastewater of coal and biomass. This approach not only facilitates the transformation of phenolic compounds but also enables their degradation into hydrogen-rich gases, thereby preventing environmental pollution and conserving energy.

In the supercritical state, water undergoes significant alterations in its physical and chemical properties, exhibiting distinctive characteristics and holding great potential for various applications. Consequently, researchers have devoted considerable attention to harnessing the exceptional properties of supercritical water, including its high diffusivity, solubility, reaction rates, and environmental friendliness. Biomass supercritical water gasification has emerged as an effective and environmentally friendly method, particularly suitable for high-moisture content feedstocks. Phenol, an essential intermediate product in

biomass supercritical water gasification, can be converted into hydrogen, carbon monoxide, carbon dioxide, methane, and other substances under appropriate supercritical water reaction conditions. However, under unfavorable conditions, the formation of undesirable compounds such as polycyclic aromatic hydrocarbons and char may occur. Therefore, it is crucial to investigate the conversion mechanism of phenol in order to optimize the process and mitigate the formation of unwanted by-products.

In the ReaxFF method developed by Van Duin et al. [11], atoms are set to be the basic unit of simulation, and the inter-atomic potential is utilized to describe the reactive events with a bond order formalism, where the bond order is empirically calculated from the inter-atomic distances. Based on the variation of the inter-atomic potential and the bond order achieved in MD simulation, the chemical reactions during the time intervals can be analyzed. In this method, the potential energy function is consisted with nine terms, as shown in Equation (1).

$$E_{\text{system}} = E_{\text{bond}} + E_{\text{over}} + E_{\text{under}} + E_{\text{val}} + E_{\text{pen}} + E_{\text{tors}} + E_{\text{conj}} + E_{\text{vdWaals}} + E_{\text{Coulomb}} \quad (1)$$

In the equation,  $E_{\text{bond}}$  represents the bond energy driven from the bond order.  $E_{\text{over}}$  and  $E_{\text{under}}$  are the over- and under-coordinated term.  $E_{\text{vdWaals}}$  stands for the van der Waals interactions, and  $E_{\text{Coulomb}}$  is the Coulombic interaction.  $E_{\text{val}}$ ,  $E_{\text{pen}}$ ,  $E_{\text{tors}}$ , and  $E_{\text{conj}}$  are the valence angle term, penalty energy term, torsion angle term, and conjugation effects, respectively.

In many contemporary studies, the combination of the ReaxFF reactive force field and density functional theory (DFT) has been employed to investigate various issues [12,13]. Ding et al. [14] investigated the solubility behaviors of polycyclic aromatic hydrocarbons (PAHs) in supercritical water through molecular dynamics simulations. The results demonstrated that PAH aggregates were relatively stable in the supercritical water/hydrogen environment, while naphthalene (NAP) aggregates were prone to rapid and complete dissolution. Li et al. [15] employed the ReaxFF MD method to study the gasification process of lignin in supercritical water, obtaining the typical pathways for the evolution of three main products ( $\text{H}_2$ ,  $\text{CH}_4$ , and  $\text{CO}_2$ ) from lignin macromolecules. Chen et al. [16] performed several sets of molecular dynamics simulations on the supercritical water gasification process of lignin. They revealed that ether bonds were initially broken during the supercritical process, and the formation of  $\text{CO}_2$  occurred in three main steps. The scale of the reaction system, reaction temperature, reactant concentration, and supercritical water density all influenced the gasification of lignin in supercritical water. In the investigation of chemical reactions, large-scale systems, and interactions involving numerous reactive sites, ReaxFF presents advantages. DFT excels in providing accurate electronic structural information and serves as a crucial tool for studying electronic properties, spectroscopy, and molecular energetics. Researchers often synergize these methods to comprehensively understand intricate molecular systems. Therefore, in this paper, we employ a combined approach of the ReaxFF reactive force field and density functional theory (DFT) to explore the mechanistic details of phenol hydrogenation via gasification in supercritical water.

## 2. Computational Method

The decomposition and gasification processes of phenol in supercritical water were investigated in this study using a combined approach of Density Functional Theory (DFT) [2,4,17] and ReaxFF [18]. The research was conducted using the Amsterdam Density Functional (ADF) software provided by SCM Corporation. The phenol model and water model were optimized using the ADF [19,20] module in the AMS 2022 software, and the optimization simulation process is illustrated in Figure 1. Additionally, to examine the reaction mechanism in detail, two reaction systems were designed, as shown in Table 1.

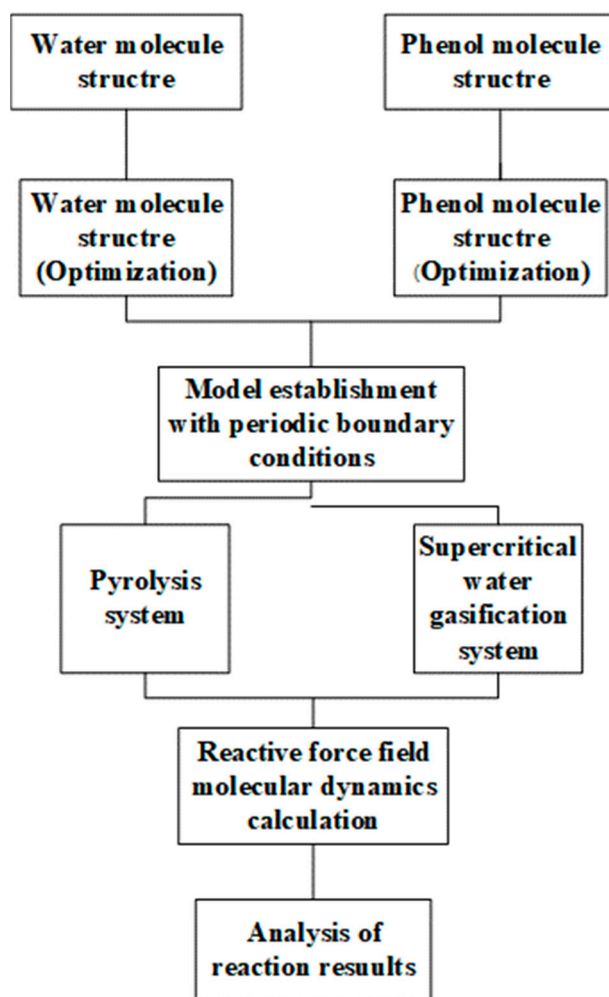


**Figure 1.** Flowchart of the optimization simulation process.

**Table 1.** Parameter configuration for two systems.

System	Phenol (Molecules)	Water (Molecules)	Pressure (MPa)	Temperature (K)
Pyrolysis	100	0	0.1	3000
Supercritical water gasification	100	500	25	3000

The initial structures of the two systems were established using the ReaxFF module in the AMS software. To eliminate potential surface effects, periodic boundary conditions [21–23] were applied to the three-dimensional models. Due to the limitations of computational simulation time, researchers often select temperatures significantly higher than those used in experiments for simulation purposes. Feng et al. [24] investigated the pyrolysis process of phenol at various temperatures and compared the distribution of reaction products. They concluded that high temperature does not influence the reaction pathway. Therefore, to ensure the smooth progression of the reaction within the simulation time, a temperature of 3000 K was chosen for the simulation.

Prior to initiating the reaction, a geometry relaxation [25–27] was performed on the entire system. The temperature was increased to the specified value at a specific rate, and the NVT ensemble (where the number of atoms, volume, and temperature remain constant) was employed. The system obtained from the NVT-EM (Energy Minimization) simulation served as the initial model for subsequent simulations. An NPT ensemble (where the

number of atoms, pressure, and temperature remain constant) was used for 500 ps, and all simulation time steps were set to 0.25 fs. Finally, in the conclusion process below, the carbon conversion rate and hydrogen conversion rate are calculated using the following formulas:

$$X (\%) = M_{C_i} + M_{C_j} / M_{C_N} \times 100\%$$

(X (%) represents the conversion rate of the corresponding element, where  $M_{C_i}$  and  $M_{C_j}$ , respectively, denote the mass of the corresponding element in the product, and  $M_{C_N}$  represents the total mass of the corresponding element.)

### 3. Results

#### 3.1. The Comparison between Pyrolysis and Supercritical Water Gasification Systems

The superiority of supercritical water was discussed by comparing the gas yields of the two systems. The variation in the number of H<sub>2</sub> molecules with reaction time is depicted in Figures 2 and 3. Figure 4 is generated by extracting the H<sub>2</sub> gas curves from Figures 2 and 3. The results clearly demonstrate that supercritical water gasification effectively enhances H<sub>2</sub> production compared to pyrolysis. Furthermore, when compared to the conditions of supercritical water gasification, pyrolysis conditions result in a higher level of tar formation during the reaction process, these tars include C<sub>6</sub>H<sub>5</sub>O, C<sub>6</sub>H<sub>7</sub>O, C<sub>6</sub>H<sub>6</sub>, C<sub>12</sub>H<sub>11</sub>O<sub>2</sub>, C<sub>12</sub>H<sub>10</sub>O<sub>2</sub>, C<sub>12</sub>H<sub>12</sub>O<sub>2</sub>, C<sub>6</sub>H<sub>7</sub>O<sub>2</sub>, C<sub>6</sub>H<sub>5</sub>, C<sub>12</sub>H<sub>9</sub>O<sub>2</sub>, C<sub>12</sub>H<sub>13</sub>O<sub>2</sub>, and so on. In their comprehensive review, M. Cortazar et al. [28] mentioned that the generation of tar leads to pipeline blockage, downstream corrosion, and catalyst deactivation, as well as adverse impacts on health and the environment. These factors severely hinder the commercialization of biomass gasification technology.

Moreover, based on the energy and temperature variations depicted in Figures 5 and 6, it can be observed that the overall temperature changes in both systems during the reaction process exhibit similarities. However, a significant disparity exists between the energy changes under pyrolysis conditions and supercritical water gasification conditions. The final energy of the pyrolysis system is approximately −231 Eh, while the energy of the supercritical water gasification system is approximately −396 Eh. According to the principles of Gibbs free energy [29], it is well known that under constant temperature and pressure conditions, a system tends to minimize its free energy and spontaneously proceed towards a state of lower energy. Notably, the energy value ΔG1 in the supercritical water state is smaller than the energy value ΔG2 in the pyrolysis state. Thus, it can be concluded that the reaction of phenol is more favorable in the supercritical state.

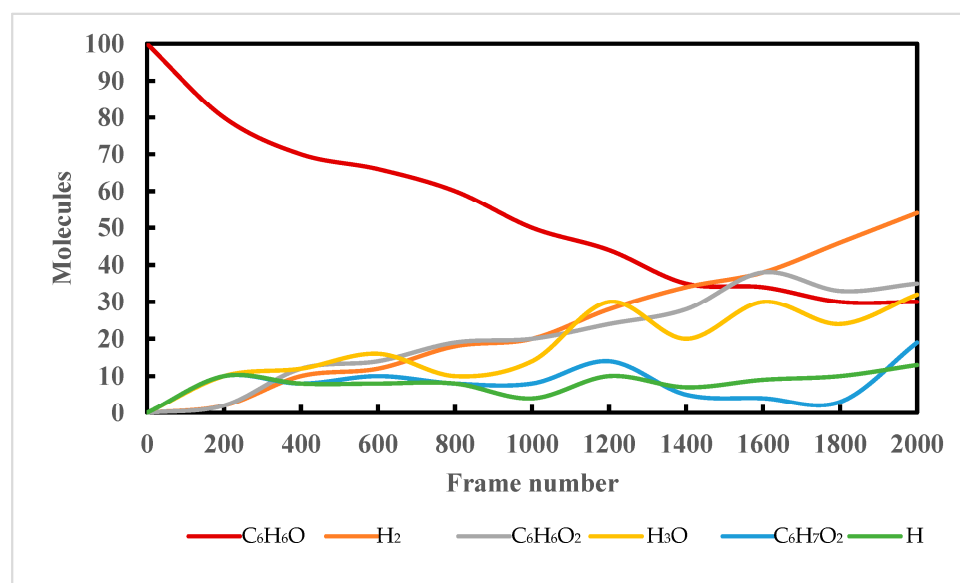


Figure 2. The temporal evolution of the predominant molecular species in SCW.

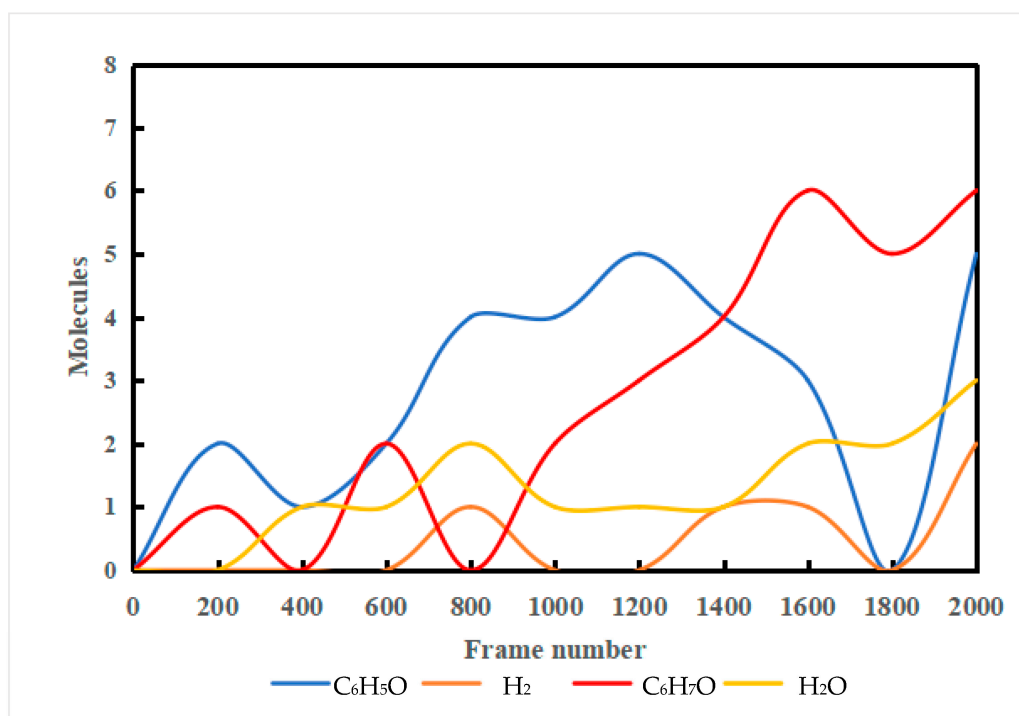


Figure 3. The temporal evolution of the predominant molecular species in pyrolysis.

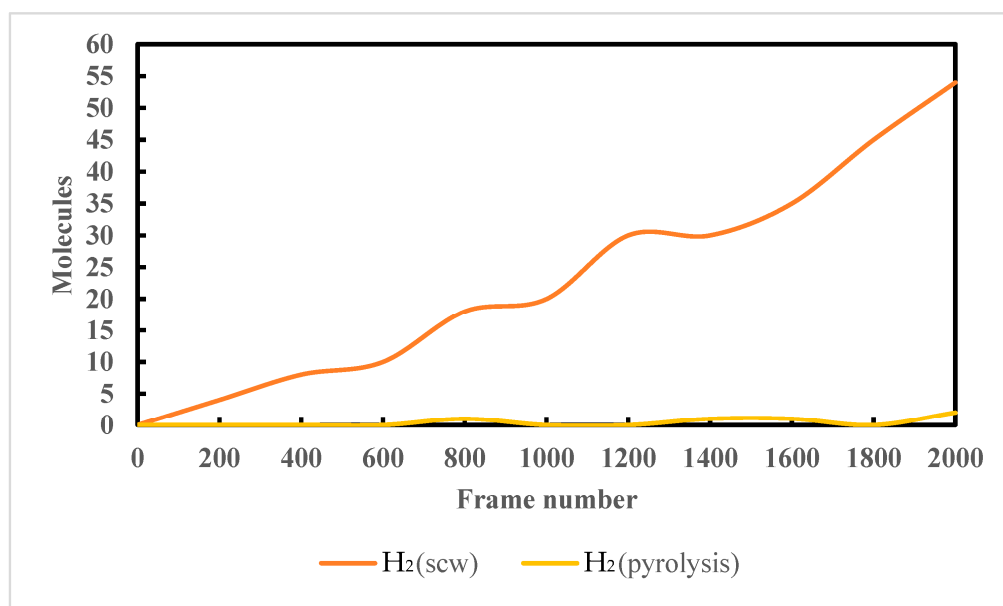
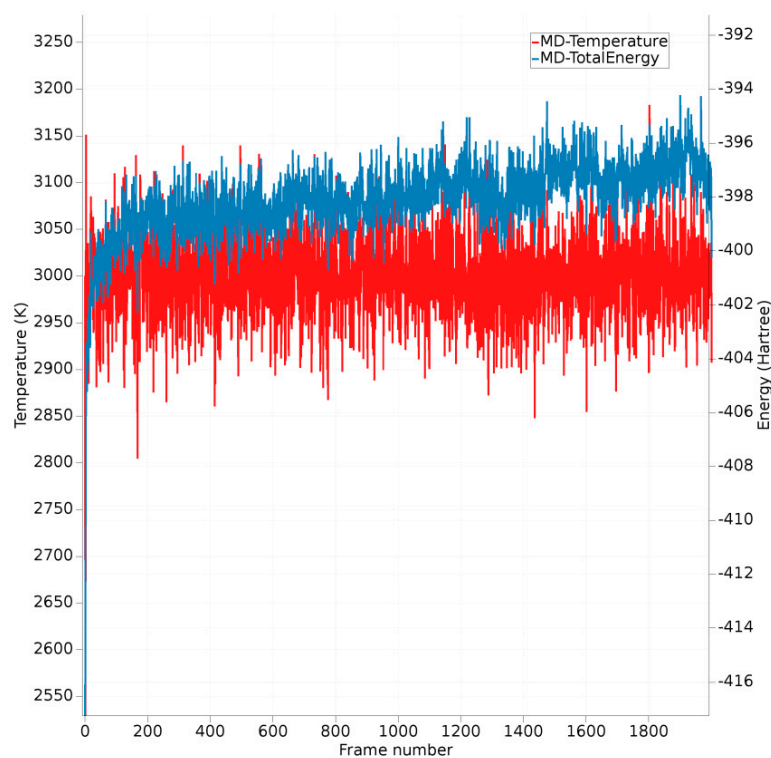
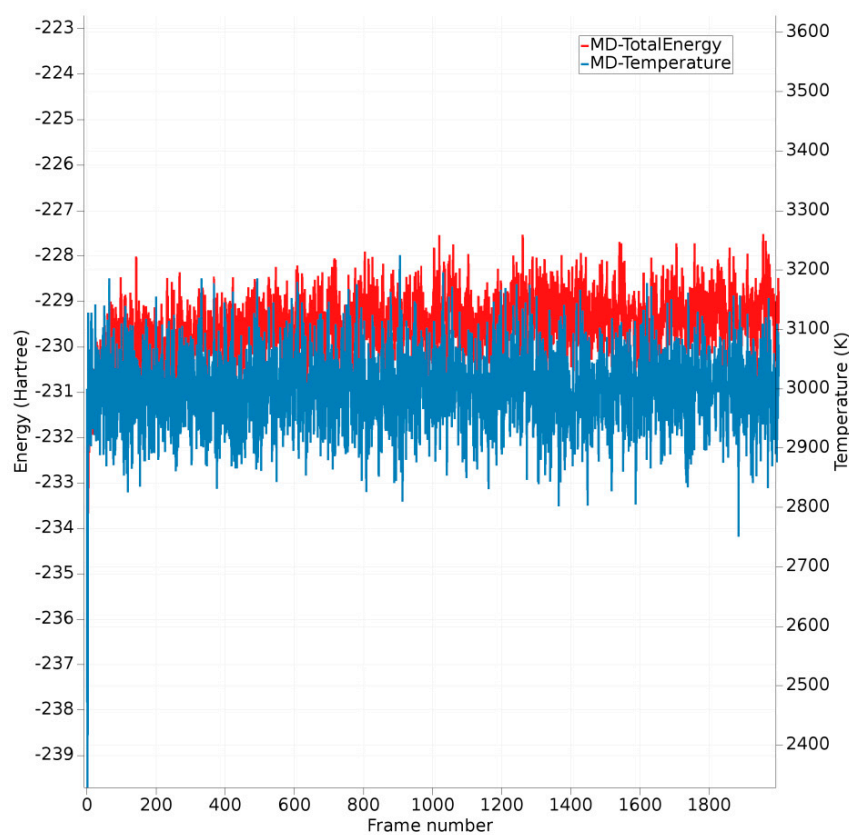


Figure 4. Abundance curves of H<sub>2</sub> were simulated in two different systems.



**Figure 5.** The relationship between temperature and total energy change in SCW.



**Figure 6.** The relationship between total energy and temperature variation during pyrolysis.

### 3.2. Product Distribution of Phenol under SCWG Conditions

The main products obtained from the 500 ps ReaxFF molecular dynamics simulation of phenol supercritical water gasification are presented in Tables 2 and 3. The tables reveal that

the major products are H<sub>2</sub>, C<sub>6</sub>H<sub>6</sub>O<sub>2</sub>, and H<sub>3</sub>O, along with C<sub>6</sub>H<sub>7</sub>O<sub>2</sub>, H, and C<sub>6</sub>H<sub>7</sub>O. Based on the calculations, after 500 ps of molecular dynamics simulation, these six products account for approximately 83.3% of the total product yield, with H<sub>2</sub> comprising 54 molecules. Conversely, the major products obtained from the 500 ps ReaxFF molecular dynamics simulation of phenol pyrolysis gasification are illustrated in the figure below. The table demonstrates that under these conditions, the main products are C<sub>6</sub>H<sub>7</sub>O, C<sub>6</sub>H<sub>5</sub>O, C<sub>12</sub>H<sub>11</sub>O<sub>2</sub>, H<sub>2</sub>O, C<sub>12</sub>H<sub>10</sub>O<sub>2</sub>, and H<sub>2</sub>. Despite having the same reactant molecules, the pyrolysis process yields only two molecules of H<sub>2</sub>. Meanwhile, we determined the carbon conversion rate and hydrogen conversion rate of the main products in both systems by employing calculation formulas, referencing Tables 1 and 2. In the pyrolysis system, the carbon conversion rate of the main products was calculated to be 23%, while the hydrogenation rate was also determined to be 23%. In the supercritical water system, the carbon conversion rate of the main products was 62%, and the hydrogenation rate of the main products throughout the entire reaction system was 38.5%.

**Table 2.** The number of major reaction product molecules in a supercritical system.

Products	Numbers (Molecules)	Percentage
H <sub>2</sub>	54	4.1129%
C <sub>6</sub> H <sub>6</sub> O <sub>2</sub>	35	3.3814%
H <sub>3</sub> O	32	3.1259%
C <sub>6</sub> H <sub>7</sub> O <sub>2</sub>	19	1.3013%
H	13	0.6165%
C <sub>6</sub> H <sub>7</sub> O	8	0.3695%

**Table 3.** The number of major reaction product molecules in a pyrolysis system.

Products	Numbers (Molecules)	Percentage
C <sub>6</sub> H <sub>7</sub> O	6	1.8160%
C <sub>6</sub> H <sub>5</sub> O	5	2.1380%
C <sub>12</sub> H <sub>11</sub> O <sub>2</sub>	3	0.8288%
H <sub>2</sub> O	3	0.8157%
C <sub>12</sub> H <sub>10</sub> O <sub>2</sub>	3	0.7277%
H <sub>2</sub>	2	0.5572%

#### 4. Conclusions

Phenol is considered an important intermediate product in biomass supercritical water gasification, and studying the conversion mechanism of phenol is of significant importance. In this study, a combined approach of reactive force field and density functional theory was employed to investigate the supercritical water gasification process of phenol. The main findings are summarized as follows:

The efficiency of phenol conversion to hydrogen in the supercritical water system is approximately 27 times higher compared to hydrogen production via pyrolysis during gasification.

Under the same experimental conditions, the carbon conversion rate and hydrogenation rate of the major products in the pyrolysis system were determined to be 23% and 23%, respectively. In contrast, in the supercritical system, the carbon conversion rate and hydrogenation rate of the major products were measured to be 62% and 38.5%, respectively.

The energy in the supercritical system is approximately half that in the pyrolysis system, favoring the ring-opening reactions of phenol and promoting hydrogen production.

The pyrolysis system produces a higher amount of aromatic compounds, as indicated by the predominant presence of four aromatic compounds among the top five products. These aromatic compounds can ultimately lead to tar formation.

**Author Contributions:** Conceptualization, Z.L. and L.Y.; methodology, Z.L.; software, Y.Q. and F.L.; formal analysis, Z.L. and L.W.; investigation, Z.L.; resources, L.Y.; data curation, L.W., Y.Q. and F.L.; writing—original draft preparation, Z.L.; writing—review and editing, L.Y.; visualization, Z.L.; supervision, B.C.; project administration, B.C.; funding acquisition, Z.L. and L.Y. All authors have read and agreed to the published version of the manuscript.

**Funding:** This work is supported by the Foundation of Jiangxi Provincial Department of Education (GJJ2200808), Key technology projects of Jiangxi Province’s major scientific and technological research and development project “unveiling and commanding” (20223AAG01009), National Natural Science Foundation of China project (52206202) and Science and technology innovation project for carbon peak, carbon neutrality of Jiangxi Carbon Neutralization Research Center (No. 2022JXST02).

**Conflicts of Interest:** The authors declare no conflict of interest.

## References

1. Berrang-Ford, L.; Ford, J.D.; Paterson, J. Are we adapting to climate change. *Glob. Environ. Chang.* **2011**, *21*, 25–33. [[CrossRef](#)]
2. Samanta, P.K.; Kim, D.; Coropceanu, V.; Brédas, J.L. Up-conversion intersystem crossing rates in organic emitters for thermally activated delayed fluorescence: Impact of the nature of singlet vs triplet excited states. *J. Am. Chem. Soc.* **2017**, *139*, 4042–4051. [[CrossRef](#)]
3. Field, C.B.; Campbell, J.E.; Lobell, D.B. Biomass energy: The scale of the potential resource. *Trends Ecol. Evol.* **2008**, *23*, 65–72. [[CrossRef](#)]
4. Olivier, Y.; Yurash, B.; Muccioli, L.; D’Avino, G.; Mikhnenko, O.; Sancho-Garcia, J.C.; Adachi, C.; Nguyen, T.Q.; Beljonne, D. Nature of the singlet and triplet excitations mediating thermally activated delayed fluorescence. *Phys. Rev. Mater.* **2017**, *1*, 075602. [[CrossRef](#)]
5. Wang, Q.; Zhang, X.; Cui, D.; Bai, J.; Wang, Z.; Xu, F.; Wang, Z. Advances in supercritical water gasification of lignocellulosic biomass for hydrogen production. *J. Anal. Appl. Pyrolysis* **2023**, *170*, 105934. [[CrossRef](#)]
6. Yin, Z.; Fu, C.; Hua, K.; Li, Y.; Gao, M.; He, S.; Ying, Q.; Qi, J. Research Overview of Biomass Hydrogen Production Technology. *Therm. Power Gener.* **2022**, *51*, 37–48.
7. Omoriyekomwan, J.E.; Tahmasebi, A.; Yu, J. Production of phenol-rich bio-oil during catalytic fixed-bed and microwave pyrolysis of palm kernel shell. *Bioresour. Technol.* **2016**, *207*, 188–196. [[CrossRef](#)]
8. Nabgan, W.; Nabgan, B.; Abdullah, T.A.T.; Ngadi, N.; Jalil, A.A.; Hassan, N.S.; Izan, S.M.; Luong, W.S.; Abdullah, S.N.; Majeed, F.S.A. Conversion of polyethylene terephthalate plastic waste and phenol steam reforming to hydrogen and valuable liquid fuel: Synthesis effect of Ni–Co/ZrO<sub>2</sub> nanostructured catalysts. *Int. J. Hydrogen Energy* **2020**, *45*, 6302–6317. [[CrossRef](#)]
9. Mosayebi, A. The kinetic and experimental study of the phenol steam reforming towards hydrogen production over Ni-Rh/MgO catalyst. *Fuel* **2023**, *334*, 126711. [[CrossRef](#)]
10. Zhang, D.; Wang, S.; Feng, Y.; Wang, Z.; Jin, H. ReaxFF-MD simulation investigation of the degradation pathway of phenol for hydrogen production by supercritical water gasification. *Energy Storage Sav.* **2023**, *in press*. [[CrossRef](#)]
11. Van Duin, A.C.T.; Dasgupta, S.; Lorant, F.; Goddard, W.A. ReaxFF: A reactive force field for hydrocarbons. *J. Phys. Chem. A* **2001**, *105*, 9396–9409. [[CrossRef](#)]
12. Xu, F.; Liu, H.; Wang, Q.; Pan, S.; Zhao, D.; Liu, Q.; Liu, Y. ReaxFF-based molecular dynamics simulation of the initial pyrolysis mechanism of lignite. *Fuel Process. Technol.* **2019**, *195*, 106147. [[CrossRef](#)]
13. Feng, W.; Li, Z.; Gao, H.; Wang, Q.; Bai, H.; Li, P. Understanding the molecular structure of HSW coal at atomic level: A comprehensive characterization from combined experimental and computational study. *Green Energy Environ.* **2021**, *6*, 150–159. [[CrossRef](#)]
14. Ding, W.; Shi, J.; Wei, W.; Cao, C.; Jin, H. A molecular dynamics simulation study on solubility behaviors of polycyclic aromatic hydrocarbons in supercritical water/hydrogen environment. *Int. J. Hydrogen Energy* **2021**, *46*, 2899–2904. [[CrossRef](#)]
15. Li, H.; Xu, B.; Jin, H.; Luo, K.; Fan, J. Molecular dynamics investigation on the lignin gasification in supercritical water. *Fuel Process. Technol.* **2019**, *192*, 203–209. [[CrossRef](#)]
16. Chen, J.; Wang, C.; Shang, W.; Bai, Y.; Wu, X. Study on the mechanisms of hydrogen production from alkali lignin gasification in supercritical water by ReaxFF molecular dynamics simulation. *Energy* **2023**, *278*, 127900. [[CrossRef](#)]
17. Olivier, Y.; Sancho-Garcia, J.C.; Muccioli, L.; D’Avino, G.; Beljonne, D. Computational design of thermally activated delayed fluorescence materials: The challenges ahead. *J. Phys. Chem. Lett.* **2018**, *9*, 6149–6163. [[CrossRef](#)]
18. Solomon, B.D.; Krishna, K. The coming sustainable energy transition: History, strategies, and outlook. *Energy Policy* **2011**, *39*, 7422–7431. [[CrossRef](#)]
19. Iype, E.; Hütter, M.; Jansen, A.P.J.; Nedeá, S.V.; Rindt, C.C.M. Parameterization of a reactive force field using a Monte Carlo algorithm. *J. Comput. Chem.* **2013**, *34*, 1143–1154. [[CrossRef](#)]

20. Jenkins, B.M.; Baxter, L.L.; Koppejan, J. Biomass combustion. In *Thermochemical Processing of Biomass: Conversion into Fuels Chemicals and Power*; John Wiley & Sons Ltd.: Hoboken, NJ, USA, 2019; pp. 49–83.
21. Te Velde, G.; Bickelhaupt, F.M.; Baerends, E.J.; Fonseca Guerra, C.; van Gisbergen, S.J.; Snijders, J.G.; Ziegler, T. Chemistry with ADF. *J. Comput. Chem.* **2001**, *22*, 931–967. [[CrossRef](#)]
22. Fonseca Guerra, C.; Snijders, J.G.; Te Velde, G.; Baerends, E.J. Towards an order-N DFT method. *Theor. Chem. Acc.* **1998**, *99*, 391–403. [[CrossRef](#)]
23. Liu, J.; Li, X.; Guo, L.; Zheng, M.; Han, J.; Yuan, X.; Nie, F.; Liu, X. Reaction analysis and visualization of ReaxFF molecular dynamics simulations. *J. Mol. Graph. Model.* **2014**, *53*, 13–22. [[CrossRef](#)] [[PubMed](#)]
24. Feng, H.; Sun, J.; Wu, Z.; Jin, H.; Guo, L. Investigation of recycled phenol effects on supercritical water gasification of coal using ReaxFF MD simulation. *Fuel* **2021**, *303*, 121177. [[CrossRef](#)]
25. Shchygol, G.; Yakovlev, A.; Trnka, T.; Van Duin, A.C.; Verstraelen, T. ReaxFF parameter optimization with Monte-Carlo and evolutionary algorithms: Guidelines and insights. *J. Chem. Theory Comput.* **2019**, *15*, 6799–6812. [[CrossRef](#)]
26. Skinner, J.L.; Park, K. Calculating Vibrational Energy Relaxation Rates from Classical Molecular Dynamics Simulations: Quantum Correction Factors for Processes Involving Vibration-Vibration Energy Transfer. *J. Phys. Chem. B* **2001**, *105*, 6716–6721. [[CrossRef](#)]
27. Melchionna, S.; Ciccotti, G.; Lee Holian, B. Hoover NPT dynamics for systems varying in shape and size. *Mol. Phys.* **1993**, *78*, 533–544. [[CrossRef](#)]
28. Cortazar, M.; Santamaria, L.; Lopez, G.; Alvarez, J.; Zhang, L.; Wang, R.; Bi, X.; Olazar, M. A comprehensive review of primary strategies for tar removal in biomass gasification. *Energy Convers. Manag.* **2023**, *276*, 116496. [[CrossRef](#)]
29. Chen, L.Q. Chemical potential and Gibbs free energy. *Mrs Bull.* **2019**, *44*, 520–523. [[CrossRef](#)]

**Disclaimer/Publisher’s Note:** The statements, opinions and data contained in all publications are solely those of the individual author(s) and contributor(s) and not of MDPI and/or the editor(s). MDPI and/or the editor(s) disclaim responsibility for any injury to people or property resulting from any ideas, methods, instructions or products referred to in the content.